J Ther Eng, Vol. 12, No. 1, pp. 144−155, January, 2026

Journal of Thermal Engineering
Web page info: https://jten.yildiz.edu.tr
DOI: 10.14744/thermal.0001065

Research Article

Opposition-based algorithm for the optimization of shell-and-tube heat exchangers

Elaheh KHOSRAVIAN[1], Mohammad B. AHMADI[1,*]

[1]*Department of Mathematics, Faculty of Science, Shiraz University, Shiraz, 71936, Iran*

ARTICLE INFO

Article history
Received: 23 September 2024
Revised: 27 November 2024
Accepted: 10 December 2024

Keywords:
Aspen-EDR Software;
Optimization Methods;
Optimizing Based Opposition;
Shell and Tube Heat Exchanger

ABSTRACT

Shell-and-tube heat exchangers are widely used across various industries due to their high efficiency in energy recovery, drying, and cooling processes. However, optimizing these exchangers presents significant challenges due to the discrete nature of the design variables and the complexity of the governing equations, which are discontinuous and non-differentiable. To address these challenges, metaheuristic algorithms such as Genetic Algorithm, Particle Swarm Optimization, and Differential Evolution are commonly applied. This study introduces two enhanced optimization algorithms: Opposition-Based Differential Evolution and Comprehensive Opposition-Based Learning. These methods incorporate the concept of opposition both in generating initial solutions and in iterative optimization processes, enabling the efficient identification of optimal solutions.

The optimization process focuses on key design variables, including tube diameter, shell diameter, and baffle spacing, which directly determine the complete geometry of the heat exchanger. The performance of these algorithms was evaluated across two case studies from prior research. Results showed an 18.88% improvement in cost reduction for the first case study and a 16.37% improvement for the second compared to conventional methods. Additionally, these algorithms outperformed Aspen EDR, a commercial heat exchanger design software, in identifying cost-effective and geometrically feasible solutions. Since Aspen EDR has limited modules for heat exchanger design and fails to provide solutions for complex geometries, such as helical or coiled tube configurations, the proposed algorithms offer a reliable and efficient alternative in such scenarios

This research demonstrates the potential of these enhanced optimization algorithms to overcome traditional design limitations, providing a more versatile and effective approach for designing shell-and-tube heat exchangers with improved performance and cost efficiency.

Cite this article as: Khosravian E, Ahmadi MB. Opposition-based algorithm for the optimization of shell-and-tube heat exchangers. J Ther Eng 2026;12(1):144−155.

***Corresponding author.**
*E-mail address: mbahmadi@shirazu.ac.ir

This paper was recommended for publication in revised form by Editor-in-Chief Ahmet Selim Dalkilic

INTRODUCTION

Shell-and-tube heat exchangers are extensively used across various industries, including energy recovery, drying, and cooling processes, due to their high efficiency and versatility [1].

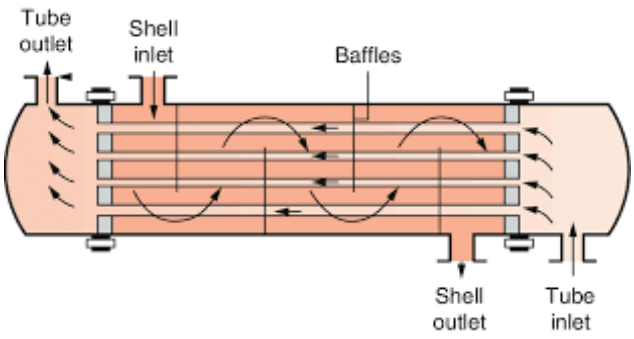

Figure 1. Shell and Tube Heat Exchanger Schematic Diagram.

However, optimizing the design of these exchangers presents significant challenges because of the discrete nature of the design variables and the complexity of the governing equations, which are discontinuous and non-differentiable [2].

Traditional optimization methods often struggle with these complexities, particularly when considering the intricate geometries and operational parameters involved in heat exchanger design. Recent studies have introduced new approaches, such as the use of nanofluids and porous media, to improve heat transfer performance and efficiency in heat exchangers. For instance, Qader et al. (2023) [3] demonstrated that using TiO2-water nanofluids in a double-pipe heat exchanger enhanced its effectiveness by incorporating porous media. Similarly, Zarda et al. (2022) [4] investigated the use of nanofluids in a flat solar collector, showcasing significant improvements in thermal efficiency through computational fluid dynamics (CFD) simulations. These studies highlight the potential of novel materials and advanced techniques for improving heat exchanger performance.

Furthermore, Hussein et al. [5] (2023) evaluated the performance of shell-and-tube heat exchangers using ZnO/water nanofluids and demonstrated notable enhancements in heat transfer rates [6]. In a similar context, Adnan Hussein et al. (2023) [6] explored the use of Fe3O4/water nanofluids in shell-and-tube heat exchangers, reporting significant improvements in heat transfer efficiency and overall performance. Qader et al. (2023) [7] also conducted a numerical study of heat transfer in circular pipes filled with porous media, emphasizing the role of advanced methodologies in optimizing heat exchanger configurations. While these methods have shown promise, they primarily focus on material innovations and fail to comprehensively address the challenges associated with optimization of complex geometries and design variables. Meanwhile, optimization techniques have also evolved to address the multi-objective nature of heat exchanger design. For example, Nadi et al. (2021) [8] employed Multi-Objective Particle Swarm Optimization (MOPSO) for the optimization of K-type shell-and-tube heat exchangers, demonstrating the potential of metaheuristic methods to balance trade-offs between thermal performance and cost. While these methods have shown promise, they primarily focus on material innovations and fail to comprehensively address the challenges associated with optimization of complex geometries and design variables.

The primary aim of this study is to introduce two advanced optimization algorithms: Opposition-Based Differential Evolution (OBDE) and Comprehensive Opposition-Based Learning (COBL) [9]. These algorithms incorporate the concept of opposition not only in generating initial solutions but also throughout the iterative optimization process, significantly enhancing the efficiency and accuracy of the solution search [10,11]. By integrating opposition mechanisms, these algorithms avoid local optima and explore a broader solution space, thus providing more reliable optimal solutions [12,13].

The optimization process in this study focuses on critical design variables, such as tube diameter, shell diameter, and baffle spacing, which directly influence the geometry and performance of the heat exchanger. The accurate determination of these variables ensures that the final design is both cost-effective and practically feasible [14]. Despite their potential, however, existing commercial software tools like Aspen EDR have limitations, particularly when dealing with complex geometries such as helical or coiled tube configurations. Aspen EDR, which is commonly used for heat exchanger design, lacks the necessary modules for handling such intricate designs, often failing to provide solutions for these types of systems [15].

To address these limitations, the proposed optimization algorithms offer a more reliable and efficient alternative, capable of handling complex geometries and producing geometrically feasible, cost-effective solutions. In this study, the performance of the proposed algorithms was evaluated through two case studies from prior research. The results demonstrated an 18.88% improvement in cost reduction for the first case study and a 16.37% improvement for the second when compared to conventional methods [16]. Moreover, the proposed algorithms outperformed Aspen EDR in terms of both cost-effectiveness and the ability to generate geometrically feasible solutions.

This paper aims to contribute to the ongoing efforts in optimizing shell-and-tube heat exchangers by providing a novel, robust optimization technique. By incorporating these advanced algorithms, the study addresses key gaps in the current literature and offers a solution that not only improves design efficiency but also opens new avenues for solving complex heat exchanger design problems. The

proposed algorithms offer significant potential for future research and practical applications, especially in industries where customized heat exchanger designs are critical for achieving optimal performance [17].

The structure of this article is organized as follows: Section 2 outlines the mathematical relationships and equations central to STHE modeling. Section 3 provides a comprehensive overview of OBL and its integration into metaheuristic frameworks. Section 4 presents the optimization results of a case study, comparing the proposed algorithms with traditional approaches. Finally, Section 5 summarizes the findings and contributions of this research.

MATHEMATICAL MODEL OF SHELL-AND-TUBE HEAT EXCHANGER

The Kern methodology, derived from research conducted at the University of Delaware [18], offers a semi-analytical framework for modeling the performance of STHEs. This approach integrates principles of fluid mechanics with the physical characteristics of STHEs, including their geometric configurations and operating conditions, to provide a comprehensive analysis of their behavior. A concise overview of this methodology is provided in the subsequent sections. The heat transfer coefficient in tube side, i.e. h_t is calculated according to the flow regime on the tube side, as given in the equations (1). The correlation is determined using the Reynolds number on the tube side.

$$h_t=\begin{cases}\frac{k_t}{d_i}\times\left[3.657+\frac{0.0677\left(\mathrm{Re}_t\times\mathrm{Pr}_t\left(\frac{d_i}{L}\right)\right)}{1+0.1\times\mathrm{Pr}_t\times\left(\mathrm{Re}_t\left(\frac{d_i}{L}\right)\right)}\right] & if \quad \mathrm{Re}_t<2300\\ \frac{k_t}{d_i}\times\left[\frac{\frac{f_t}{8}(\mathrm{Re}_t-1000)\times\mathrm{Pr}_i)}{1+12.7(\frac{f_t}{8})\times(\mathrm{Pr}_t^{\frac{2}{3}}-1)}\times(1+\frac{d_i}{L})^{0.67}\right] & if \quad 2300\le Re_t\le 10000\\ 0.027\frac{k_t}{d_o}Re_t^{0.8}\,Pr_t^{\frac{1}{3}}\left(\frac{\mu_t}{\mu_{wt}}\right)^{0.14} & if \quad Re_t>10000\end{cases} \quad (1)$$

The equations governing the problem as well as the required parameters are given in the Table 1.

Table 1. System Equations and Parameters [16]

	Symbol	
Darcy friction factor tube side	f_t	$f_t=(1.82\times log_{10}Re_t-1.64)^{-2}$
Darcy friction factor in shell side	f_s	$f_s=2b_o\,Re_s^{-0.15}$
Coefficient of heat transfer in shell side	h_s	$h_s=0.36\frac{k_s}{d_e}Re_s^{0.55}\,Pr_s^{\frac{1}{3}}\left(\frac{\mu_t}{\mu_{ws}}\right)^{0.14}$
Prandtl number in tube side	Pr_t	$Pr_t=\frac{\mu_t Cp_t}{k_t}$
Heat transfer rate	Q	$Q=m_hC_{ph}(T_{hi}-T_{ho})=m_sC_{pc}(T_{co}-T_{ci})$
Reynolds number in shell side	Re_s	$Re_s=\frac{m_sd_e}{A_s\mu_s}$
Reynolds number in tube side	Re_t	$Re_t=\frac{m_sd_e}{A_s\mu_s}$
Fluid velocity in shell side (m/s)	v_s	$v_s=\frac{m_s}{\rho_sA_s}$
Fluid velocity in tube side (m/s)	v_t	$v_t=\frac{\dot{m}_t}{\frac{\pi}{4}{d_i}^2\rho_t}(\frac{n}{N_t})$
Pressure drop (Pa)	ΔP	
Tube side pressured drop	ΔP_t	$\Delta P_t=\frac{\rho_tv_t^2}{2}(\frac{L}{d_i}\times f_t+p)\times n$
Shell side pressured in Kern's method	ΔP_s	$\Delta P_s=f_s(\frac{\rho_sv_s^2}{2})(\frac{L}{B})(\frac{D_s}{d_e})$
Diameter of shell hydraulic in square pitch arrangement	d_{es}	$d_{es}=\frac{4(S_t^2-\left(\frac{\pi d_o^2}{4}\right))}{\pi d_o}$

Table 1. System Equations and Parameters [16] (continued)

	Symbol	
Diameter of shell hydraulic in triangular pitch arrangement	d_{et}	$d_{et} = \frac{4(0.43S_t^2 - \left(\frac{0.5\pi d_o^2}{4}\right))}{0.5\pi d_o}$
Surface area of shell side	A_s	$A_s = D_s B(1 - \frac{d_o}{S_t})$
Shell side Prandtl number	Pr_s	$Pr_s = \frac{\mu_s C_{ps}}{k_s}$
Overall heat transfer coefficient (W/m2 k)	U	$U = \frac{1}{(\frac{1}{h_s}) + R_{fs} + (\frac{d_o}{d_i}) \times (R_{ft} + (\frac{1}{h_t}))}$
The logarithmic mean temperature difference (LMTD)	LMTD	$LMTD = \frac{(T_{hi} - T_{co}) - (T_{ho} - T_{ci})}{ln(\frac{T_{hi} - T_{co}}{T_{ho} - T_{ci}})}$
Correction coefficient	R	$R = \frac{T_{hi} - T_{ho}}{T_{co} - T_{ci}}$
Efficiency Factor	P_E	$P_E = \frac{T_{co} - T_{ci}}{T_{hi} - T_{ci}}$
Correction factor of flow configuration	F	$F = \sqrt{\frac{R^2+1}{R-1} \times (\frac{ln(\frac{1-p}{1-pr})}{ln(\frac{2-PR+1-\sqrt{R^2+1}}{2-PR+1-\sqrt{R^2+1}})}}$
Surface area of heat exchanger (m2)	A	$A = \frac{Q}{U \times F \times LMTD}$
Tube length (m)	L	$L = \frac{A}{\pi d_o N_t}$
Power of pumping (w)	Pw	$Pw = \frac{1}{\eta} \times (\frac{m_t}{\sigma_t} \times \Delta P_t + \frac{m_s}{\sigma_s} \times P_S)$

Definitions of parameters are summarized in Table 2.

Proposed Meta Heuristic Algorithm

This section deals with the proposed metaheuristic algorithms, i.e. OBDE and CO-OBL. Before the algorithms are presented, the cost function and some preliminaries are given below.

Cost calculation

The objective function corresponding to the total cost C_{tot} includes the annual fixed costs, i.e. C_i and the operating costs, i.e. C_{op}, is as follows:

$$C_{tot} = C_i + C_{op} \quad (2)$$

The annual fixed cost, i.e. C_i, is the function of the heat exchanger area, as shown in Eq. (3).

$$C_i = a_1 + a_2 A^{a_3} \quad (3)$$

where, both the shell and tubes were made with stainless steel and its corresponding parameters are a_1 = 8000, a_2 = 259.2, and a_3 = 0.93 [16]. The operational cost is the function of pumping power overcome friction losses and calculated by Eqs. (4) and (5).

$$C_0 = PC_eH \quad (4)$$

$$C_{op} = \sum_{x=1}^{n_y} \frac{C_o}{(1+y)^x} \quad (5)$$

The design variables including the tube outside diameter, i.e. d_o, the shell inside diameter, i.e. D_S, and the baffle spacing i.e. B are applied in the optimization method to find

Table 2. System Parameters and Design Variables

Design variable/Parameter	Symbol	Design variable/Parameter	Symbol
Constant value (€)	a_1	Fouling resistance in shell side (m2 K/W)	R_{fs}
Constant value (€/m2)	a_2	Fouling resistance in tube side (m2 K/W)	R_{ft}
Constant value	a_3	tube pitch (m)	S_t
Area of shell side (m2)	A_s	Inlet temperature of cold fluid (K)	T_{ci}
baffles spacing (m)	B	Outlet temperature of cold fluid (K)	T_{co}
Constant value	C	Inlet temperature of hot fluid (K)	T_{hi}
Cost of energy (€/kW h)	C_e	Difference in heat transfer (W/m2 K)	Δ_h
Value of clearance (m)	cL	pressure drop (Pa)	ΔP
operating cost (€)	C_{op}	dynamic viscosity (Pa s)	μ
Total cost (€)	C_{tot}	density (kg/m3)	ρ
Diameter of tube inside (m)	d_i	overall pumping efficiency	η
Diameter of tube outside (m)	d_o	cold stream	c
Diameter of shell inside (m)	D_s	Equivalent	e
operating time in annual measure (h/yr)	H	Hot stream	h
discount rate in annual measure (%)	y	Device Inlet	i
Mass flow rate in shell side (kg/s)	m_s	Device Outlet	o
Mass flow rate in tube side (kg/s)	m_t	Shell side	s
Tube passes count	n	Tube side	t
Constant value	n_1	Wall of Tube	wt
Device life (yr)	ny		

the minimum objective function. The ranges of the input parameters are as follows: tube outside diameter is between 0.010 *m* and 0.051 *m*, shell inside diameter is between 0.1 *m* and 1.5 *m*, and baffle spacing is between 0.050 *m* and 0.5 *m*.

The opposition concept

This section discusses the application of the opposite concept in optimization. Various forms of oppositions are defined in [19] and elucidating how they can be employed in optimization scenarios. Two optimization methods that leverage oppositions are delineated, offering practical insights into their implementation and efficacy [19, 20]. First, the opposite is defined and elucidating how it can be employed in optimization scenarios.

Definition 1. (Opposite number): Let x be a real number in an interval $[a,b]$. The opposite of x, denoted by $\tilde{x}$, is defined by equation (6).

$$\tilde{x} = a + b - x \tag{6}$$

Definition 2 (Opposite Point): Let $P(x_1, x_2, ..., x_D)$ be a point in d-dimensional space, where $x_1, x_2, ..., x_D$ are real numbers and $x_i \in [a_i, b_i], i = 1,2,\ldots,d$. The opposite of P is denoted by $\tilde{P}(\tilde{x}_1, \tilde{x}_2, ..., \tilde{x}_D)$, where $\tilde{x}_i = a_i + b_i - x_i, i = 1,2,\ldots,d$.

To increase the probability of obtaining better approximations of the optimal solution while controlling the diversity of candidate solutions, comprehensive opposition (*CO*) changes the value of each variable $x \in [a,b]$ to one of its opposite points $\tilde{x}^{reo}$, $\tilde{x}^{qr}$, $\tilde{x}^{qo}$, or $\tilde{x}^{eo}$, whose selection probabilities are the optimal solution of one linear parametric programming with parameters $t = T$, where t is the number of iterations and T is the total number of iterations. The associated definitions and theorems are described in [19].

The comprehensive opposition concept serves as the primary operator in opposition-based optimization (OBA), enhancing the candidate solutions while regulating their variability.

Definition 3 (Comprehensive opposite point): Let $\tilde{x}^{qo}$, $\tilde{x}^{qr}$, $\tilde{x}^{eo}$, $\tilde{x}^{reo}$ be the Quasi-opposite (Quasi-opposition, shifts the amount of each variable to a random point between the center of its domain and its opposite number), Quasi-reflected (Quasi-reflection, reflects the amount of each variable x to a random point between the center of its domain and *X*), Extended opposite (Extended opposition shifts the amount of each variable to a random point between its opposite number and the nearest bound of its domain to its opposite number), and Reflected Extended opposite (Reflected extended opposition reflects the extended opposite point to obtain the reflected extended opposite point) point of v, respectively. The comprehensive opposite point of X is denoted by $\tilde{X}^{co}$ $(\tilde{x}_1^{co}, \tilde{x}_2^{co}, ...\tilde{x}_d^{co})$ and defined for t-th iteration as follows:

if $0 < \frac{t}{T} \leq \frac{43}{192}$

$$\tilde{X}_i^{co} = \begin{cases} \tilde{x}_i^{reo}, rand_i \le 0.01 \\ \tilde{x}_i^{qr}, 0.01 \le rand_i \le 0.02 \\ \tilde{x}_i^{qo}, 0.02 \le rand_i \le 0.56 + 1.92\frac{t}{T} \\ \tilde{x}_i^{eo}, 0.56 + 1.92\frac{t}{T} \le rand_i \le 1 \end{cases} \quad (7)$$

else

$$if\ \frac{43}{192} < \frac{t}{T} \le \frac{139}{192}$$

$$\tilde{X}_i^{co} = \begin{cases} \tilde{x}_i^{reo}, rand_i \le 0.01 \\ \tilde{x}_i^{qr}, 0.01 \le rand_i \le -0.42 + 1.92\frac{t}{T} \\ \tilde{x}_i^{qo}, -0.42 + 1.92\frac{t}{T} \le rand_i \le 0.96 \\ \tilde{x}_i^{eo}, 0.96 \le rand_i \le 1 \end{cases}$$

else

$$\tilde{X}_i^{co} = \begin{cases} \tilde{x}_i^{reo}, & rand_i \le 0.01 \\ \tilde{x}_i^{qr}, & 0.01 \le rand_i \le 0.02 \\ \tilde{x}_i^{qo}, & 0.02 \le rand_i \le 0.03 \\ \tilde{x}_i^{eo}, & 0.03 \le rand_i \le 1 \end{cases},$$

where, $1 \le i \le$ d, T is the total number of iterations, and $rand_i$ is a random number uniformly distributed in $[a,b]$. The above opposite points have already been defined by the authors of this paper in detail in [19]. Also, Theorems with their corollaries prove that the comprehensive opposite point is more effective than the independent random point [19].

Opposition-Based Differential Evolution (OBDE)

Like other population-based optimization algorithms, Differential Evolution (DE) operates through two primary stages: (i) initialization of the population and (ii) generation of a new population via evolutionary operations, including mutation, crossover, and selection. The objective of this study is to enhance these stages by incorporating opposition-based optimization principles. The classical DE serves as the foundational algorithm, which is augmented with the proposed optimization strategies to achieve improved convergence speed.

In alignment with standard population-based algorithms, the core stages of DE—population initialization and the generation of new individuals through evolutionary mechanisms—are systematically refined through the integration of opposition-based optimization principles. This integration aims to enhance the algorithm's efficiency and robustness in navigating complex search spaces.

The corresponding pseudocode and block diagram for the proposed method (OBDE) are provided in Algorithm 1 [13]. The main steps of Algorithm 1 are discussed in detail below.

Step 1. Initialize the population $P(N_P)$ randomly.

Step 2. Calculate opposite population by

$$OP_{i,j} = a_j + b_j - P_{i,j}$$
$$i = 1,2,\ldots,N_p, j = 1,2,\ldots,D \quad (9)$$

Where, $P_{i,j}$ and $OP_{i,j}$ denote the j^{tj} variable of the i^{tj} population and the opposite population vector, respectively.

Step 3. Select the N_P fittest individuals from the set $\{P \cup OP\}$ as the initial population. According to the above procedure, $2N_P$ function evaluations are required instead of the $2N_P$ conventional random population initialization. However, with the opposition-based initialization, these algorithms can commence with more suitable initial individuals.

The DE is effective for high-dimensional problems and OBDE exhibits superior performance with larger population sizes. Moreover, a jumping rate range of [0.1; 0.4] is proposed for the STHE optimization problem.

Algorithm 1: OBDE scheme (N_P, J_r, *MAX - NFC*)

1. N_P, J_r, and *MAX - NFC* are the population size, jumping rate, and the maximum number of the cost function evaluations, respectively.
2. Opposition-Based Population Initialization.
3. Generating the initial population uniform randomly, *pop*.
4. Calculating the opposite population, *opop* by Eq. (9).
5. Picking N_P fittest solutions from *pop*∪*opop* as the initial population.
6. *NFC* = 1.
7. while *NFC* < *MAX - NFC* do
8. Mutation
9. Crossover
10. Selection
11. Opposition-Based Jumping
12. if *rand* (0,1) < J_r then
13. *rand* (0,1) Generates a random number in [0,1].
14. Calculating opposite population of current population, *opop*(*NFC*) by Eq. (9).
15. *NFC* = *NFC* + N_P
16. Picking N_P fittest solutions from *pop*∪*opop* as the current population.
17. end if
18. *NFC* = *NFC* + N_P.
19. end while

Comprehensive Opposition-Based Learning (CO-OBL)

As mentioned, the opposition-based algorithm is a population-based stochastic metaheuristic optimization algorithm for optimization problems. The superiority of this algorithm is its simplicity, low computational burden speed, and fast convergence in obtaining the optimal solution. To increase the probability of obtaining better approximations of the optimal solution while controlling the diversity of candidate solutions, comprehensive opposition (*CO*) modifies the value of each variable in $x \in [a,b]$ to one of its opposite points $\tilde{x}^{qo}$, $\tilde{x}^{qr}$, $\tilde{x}^{eo}$, $\tilde{x}^{reo}$, the probabilities to

Table 3. Case studies parameters

		$\rho\ (kg/m^3)$	$C_p\ (KJ/KgK)$	$\mu\ (PaS)$	$K\ (W/mK)$	$R_f\ (m^2K/W)$
Case 1						
	Shell side	750	2.84	0.00034	0.19	0.00033
	Tube side	995	4.2	0.0008	0.59	0.0002
Case 2						
	Shell side	1000	4.187	0.00071	0.63	7 × 10^4
	Tube side	656	2.646	0.00037	0.11	7 × 10^4

be selected are the optimal linear parametric programming solution with parameter $t = T$ where t is the number of iterations and T is the total number of iterations. The different steps of the proposed algorithm are outlined as follows [19]:

Algorithm 2: CO-OBL.

1. (Random initialization) Generate a random population P with N points.
2. (Fitness evaluation of points) Evaluate the fitness of each point.
3. Calculate the comprehensive opposite population P^{Co}.
4. Update the population P by selecting N potentially useful solutions from the set $P^{Co} \cup P$.
5. Update $X^{best}(t)$ $best(t)$, $worst(t)$, $P_m^i(t)$ and for $i = 1,2, \ldots, N$.
6. Replace the point X^i of the population with its current optimum opposite point, X^{iCo} with the probability $P_m^i(t)$ and for $i = 1,2, \ldots, N$.

$$P_m^i(t) = (best(t) - fit^i(t))/(best(t) - worst(t)) \quad (10)$$

7. Repeat Steps 2–6 until the stopping criterion is met.

Simulation Results

The numerical experiments were carried out on a computer equipped with an Intel i7 processor, 16 GB RAM, a 6 GB graphics card, and the Windows 7 64-bit operating system, using MATLAB R2014b.A.

Case studies

This study evaluates the performance of the proposed optimization algorithms through two case studies, as reported by Caputo et al. [21]. In both cases, the thermophysical properties of the working fluids are computed at their mean temperatures. The first case study involves methanol on the shell side, with a flow rate of 27.8 kg/s and inlet and outlet temperatures of 95 °C and 40 °C, respectively. On the tube side, seawater is utilized with a flow rate of 68.9 kg/s, entering at 25 °C and exiting at 40 °C. Both the shell and tube components are constructed from stainless steel.

Case study 2 consists of cooling water placed in the shell side with the flow rate of 30 kg/s and the inlet and outlet temperatures of 33 °C and 37 °C, respectively. Naphtha is in the tube side with the flow rate of 2.70 kg/s and the inlet and outlet temperatures of 114 °C and 40 °C, respectively. Stainless steel is used as a construction material for shell and tubes. The other parameters for these case studies are given in Table 2. The second case study examines the use of cooling water on the shell side, characterized by a flow rate of 30 kg/s and inlet and outlet temperatures of 33 °C and 37 °C, respectively. On the tube side, naphtha is employed as the working fluid, with a flow rate of 2.70 kg/s, entering at 114 °C and exiting at 40 °C. Like the first case study, stainless steel is used as the material for both the shell and tube components. Additional parameters for these case studies are summarized in Table 3[16].

RESULTS AND DISCUSSION

The proposed algorithms, Opposition-Based Differential Evolution (OBDE) and Comprehensive Opposition-Based Learning (CO-OBL), offer significant advancements in optimizing shell-and-tube heat exchangers (STHE). Their capability to minimize total costs while enhancing design efficiency showcases their robustness and practicality for addressing complex optimization challenges. Below, the key findings, comparisons, and implications of these results are discussed in detail.

Performance Comparison with Metaheuristic Methods

The proposed OBDE and CO-OBL algorithms outperform several existing metaheuristic methods, including PSO, GWO, and NSGA-II PSO. For instance, as shown in Table 4 (Case Study 1), OBDE and CO-OBL achieved a 16.37% reduction in total cost compared to NSGA-II PSO. Similarly, in Table 5 (Case Study 2), the proposed algorithms reduced costs by 18.88%. These improvements highlight the efficiency of the opposition-based strategies in finding globally optimal solutions where conventional methods may converge to suboptimal local minima.

Advantages of the Proposed Algorithms Over Aspen-EDR

The results presented in Table 3 indicate that the opposition-based algorithms (OBDE and CO-OBL) outperform Aspen-EDR, even in scenarios where the software can provide solutions. This is a significant and positive finding, as it validates the reliability of the proposed algorithms and supports the claim that they can be effectively employed

Table 4. Performance Comparison in Case Study 1[16]

Parameters	PSO	I-ITHS	CI	ARGA	NSGA II -PSO	GWO	OBDE	CO-OBL	Aspen-EDR
D_s	0.81	0.763	0.78	0.665	1.5	0.565	0.5126	0.5126	0.5906
L	3.115	2.039	1.936	1.263	0.438	7.6734	4.8622	4.8622	4.8768
B	0.424	0.495	0.5	0.49	0.416	0.3962	0.4397	0.4397	0.387
d_o	0.015	0.01	0.01	0.01	0.0139	0.0216	0.015	0.015	0.015
n	2	2	2	2	2	2	2	2	2
N_t	1658	3558	3734.12	2625.873	7628	276	604	604	742
v_t	0.67	0.7744	0.738	1.049	0.1662	2.1399	2.0162	2.0162	1.78
Re_t	10,503	7701.29	7342.74	10,440.1	2300	45984	30091	30091	20310
Pr_t	5.7	5.7	5.69	5.694	5.694	5.6949	5.6949	5.6949	5.7
h_t	3721	4388.79	4584.7	6196.002	8469	7075	7256	7256	6050
f_t	0.0311	0.03555	0.034	0.031	0.1018	0.0213	0.0236	0.0236	0.233
ΔP_t	4171	6887.63	5862.72	9756.238	1200	61404	55192	55192	036
d_e	0.0107	0.00711	0.007	0.007	0.009	0.018	0.0125	0.0125	0.0125
v_s	0.53	0.48979	0.475	0.568	0.288	0.9936	0.9135	0.9135	0.41
Re_s	12,678	7684.05	7451.39	8912.325	6300	3452	25193	25193	16450
Pr_s	5.1	5.08215	5.082	5.082	5.0821	5.0821	5.0821	5.0821	6.5
h_s	1950.8	2230.91	2195.94	2422.804	5939.2	6840	7695	7695	2876
f_s	0.349	0.37621	0.378	0.368	0.3877	0.2944	0.3149	0.3149	0.3149
ΔP_s	20,551	14,953.9	13,608.4	10,746.3	19,855	66,267	48693	48693	0.07
U	713.9	761.578	764.5	1031.472	1093.3	1107	1133	1133	1760
S	243.2	228.03	227.16	168.275	146.11	143.718	140.431	140.431	167.5
C_i	46,453	44,259.0	44,132.5	35,498.8	34,718	31,822	31,325	31,325	31,410
C_o	6778.2	5914.06	5873.66	6414.68	5161.4	2413	2025	2025	2301
C_{tot}	53,231	50,173	50,006.1	41,913.5	39,880	34,235	33350.0	33350.0	33711.0

Table 5. Performance Comparison in Case Study 2[16]

Parameters	Java Algorithm	NSGA II -PSO	OBDE	CO-OBL
D_s	0.344	0.685	0.131	0.131
L	3.22	4.71	6.5	6.5
d_o	0.015	0.015	0.015	0.015
n	1	2	2	2
N_t	186	77	23	23
ΔP_t	8450	12225	16911	16923
ΔP_s	6990	210	1013	1007
S	299.0	158.91	68.682	68.682
C_i	3660	3427	2496	2496
C_o	318	11	332	332
C_{tot}	3986	3438	2828	2828

in cases where Aspen-EDR encounters limitations. While Aspen-EDR is widely used in the industry, it has notable limitations in handling complex geometries, such as helical or coiled tube configurations, due to the absence of appropriate design modules. In such cases, OBDE and CO-OBL provide robust and reliable alternatives, delivering geometrically feasible and cost-efficient solutions.

Aspen-EDR, though widely used in industry, is limited in handling complex geometries like triangular pitch arrangements. The results in Figure 2 demonstrate that

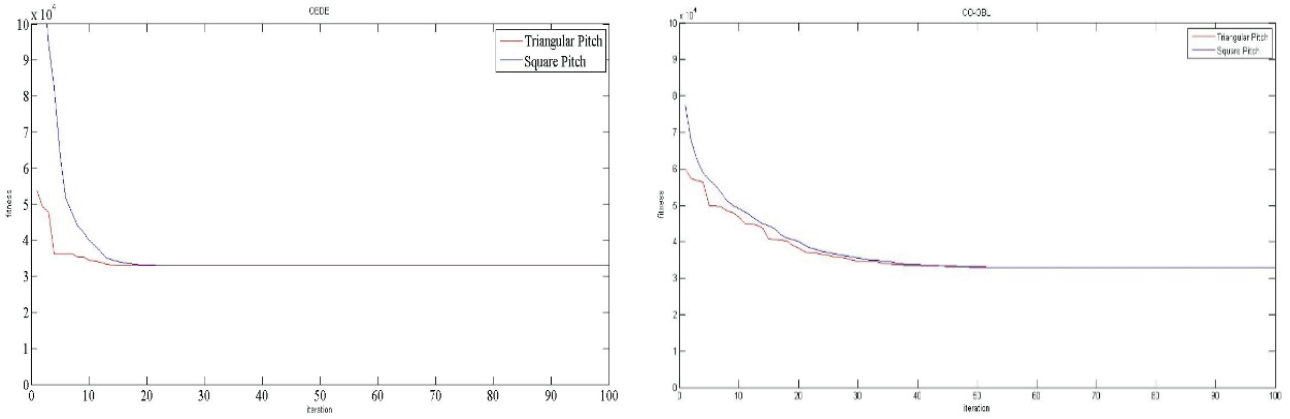

(a) (b)

Figure 2. Comparison of Triangular and Square Pitch Arrangements **(a).** OBDE and **(b).** CO-OBL.

OBDE and CO-OBL outperform Aspen-EDR by providing geometrically feasible and cost-efficient solutions for these configurations. The triangular pitch arrangement, for example, yielded approximately 2% lower costs compared to square arrangements, with significantly reduced pressure drops on both the shell and tube sides.

Advantages of Triangular Pitch Over Square Pitch Configurations

Triangular pitch arrangements have shown superior performance compared to square pitch configurations in shell-and-tube heat exchangers. As depicted in Figure 2, employing a triangular pitch configuration result in approximately 2% lower overall costs compared to square pitch designs. This cost reduction is primarily attributed to significantly reduced pressure drops on both the shell and tube sides. A detailed comparison of the pressure drops for both arrangements on the shell and tube sides is presented in Table 6. These findings highlight that triangular pitch arrangements are a more effective choice for optimizing the design of heat exchangers, and the proposed algorithms excel in identifying such optimal configurations.

Impact of Initial Population

One of the distinguishing features of OBDE is its intelligent initialization of the population. As shown in Table 7, this method achieves faster convergence (35% reduction in iterations) and lower initial costs (40% cost savings) compared to algorithms such as GSA and ACO. By leveraging opposition-based learning, OBDE effectively evaluates potential starting points during initialization, ensuring that the population begins closer to the global optimum.

The use of opposition-based learning for selecting initial points provides a distinct advantage over random initialization methods by reducing the likelihood of being trapped in local optima. By systematically exploring opposite points, the algorithm can evaluate a broader search space, leading to better initial solutions. This approach accelerates the optimization process and significantly enhances the quality of the final solutions.

Table 6. Pressure Drop Comparison for Triangular and Square Arrangements

Algorithm	ΔP_s		ΔP_t	
	S-Arrangement	T-Arrangement	S-Arrangement	T-Arrangement
DE	244320	149800	466170	414550
GA	88011	48178	215010	175400
GSA	727030	362230	2426200	1102300
GWO	46954	50553	84254	54040
PSO	192940	135910	1869800	1045300
SA	192940	135910	1869800	1045300
WOA	192940	135910	1869800	1045300
CO-OBL	48693	44188	55192	55388
OBDE	48693	44188	55192	55388

Table 7. Iteration Convergence Comparison for Case Study 1

Iteration	DE	GA	GSA	GWO	PSO	SA	WOA	CO-OBL	OBDE
1	72916	68678	73331	67840	71250	68774	67040	61756	57274
2	72916	68678	72407	62697	68783	68766	59123	61756	42220
3	68470	64531	68530	60007	64378	68560	56849	58884	42220
4	68470	59380	68086	59324	62098	68412	56849	53145	38076
5	60687	59380	67722	56530	59148	67440	56849	50501	37840
6	60687	58450	67607	49598	57781	67087	56849	50501	35689
7	60687	54784	67351	41098	57600	63660	56849	49992	35689
8	58633	54784	67059	34330	56992	63660	56849	49961	35689
9	58633	54784	66782	33912	56849	62871	56849	46379	35689
10	58443	54784	66677	33013	56849	62535	56849	46379	35689

Practical Implications

The findings underline the applicability of the proposed algorithms in industries such as energy recovery and chemical processing. By reducing costs and optimizing thermal performance, OBDE and CO-OBL enable the design of more efficient and economical heat exchangers. This adaptability to various operational conditions makes these algorithms a valuable alternative to traditional methods.

Limitations and Future Directions

While the proposed algorithms exhibit strong performance, the study is not without limitations:

Simulation-based Validation: The results are based solely on numerical simulations. Experimental validation is necessary to confirm their practicality in real-world scenarios.

Limited Case Studies: Only two case studies were analyzed. Expanding the algorithm's application to more diverse configurations, including multi-objective scenarios, could enhance its generalizability.

Scalability: Future research should investigate the algorithms' performance on larger-scale problems to assess their efficiency and adaptability.

Population size

To determine the optimal population size, a sensitivity analysis was conducted using Case Study 1. Population sizes ranging from 10 to 50 individuals were tested, with 50 iterations performed for each population size. Figure 3 illustrates the average total cost behavior for the OBDE, CO-OBL, BAT, PSO, Cuckoo Search, and DE algorithms. It was observed that the performance of these algorithms became similar when the population size exceeded 50 individuals. Consequently, a population size of 50 was selected for all optimization problems.

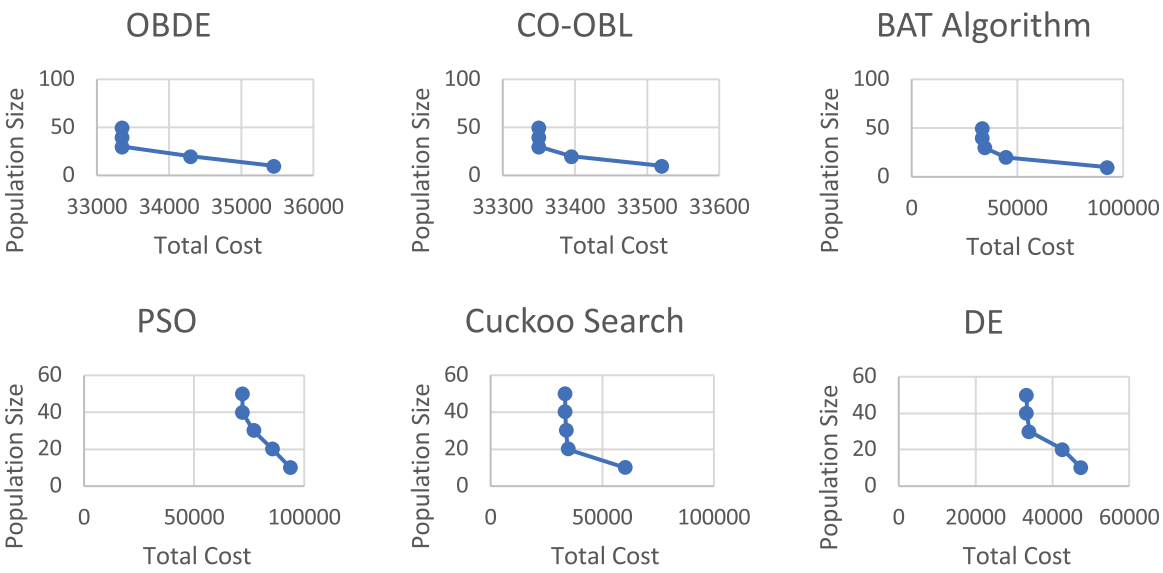

Figure 3. Population size sensitivity analysis for case study 1.

CONCLUSION

The optimization of Shell-and-Tube Heat Exchangers (STHEs) remains a critical area of research, particularly for reducing costs and enhancing performance in industrial applications. Existing methods, including traditional metaheuristic algorithms such as PSO, NSGA-II-PSO, and ARGA, often fail to escape local optima or deliver parameter configurations comparable to commercially established tools like Aspen-EDR. This study introduced two advanced algorithms, Opposition-Based Differential Evolution (OBDE) and Comprehensive Opposition-Based Learning (CO-OBL), to address these challenges effectively. By integrating the concept of opposition into both initialization and iterative optimization processes, these algorithms demonstrated superior capabilities in global exploration and solution refinement. Through two case studies, the proposed methods achieved significant cost reductions of 16.37% and 18.88% compared to NSGA-II-PSO, while maintaining design parameters consistent with Aspen-EDR. Additionally, OBDE and CO-OBL successfully optimized complex geometries, such as helical tube configurations, which are beyond the scope of conventional tools like Aspen-EDR. The results underscore the efficacy of opposition-based strategies in delivering robust, cost-effective, and geometrically feasible designs, establishing these algorithms as promising alternatives for the optimization of STHEs. Future research could focus on experimental validation, extending the application to multi-objective scenarios, and exploring scalability to large-scale industrial problems.

AUTHORSHIP CONTRIBUTIONS

Authors equally contributed to this work.

DATA AVAILABILITY STATEMENT

The authors confirm that the data that supports the findings of this study are available within the article. Raw data that support the finding of this study are available from the corresponding author, upon reasonable request.

CONFLICT OF INTEREST

The author declared no potential conflicts of interest with respect to the research, authorship, and/or publication of this article.

ETHICS

There are no ethical issues with the publication of this manuscript.

STATEMENT ON THE USE OF ARTIFICIAL INTELLIGENCE

Artificial intelligence was not used in the preparation of the article

REFERENCES

[1] Kakac S, Liu H, Pramuanjaroenkij A. Heat exchangers: selection, rating, and thermal design. 3rd ed. Boca Raton (FL): CRC Press; 2012.

[2] Kennedy J, Eberhart RC. A discrete binary version of the particle swarm algorithm. In: Proceedings of the IEEE International Conference on Systems, Man, and Cybernetics; 1997. p. 4104–4108. [CrossRef]

[3] Qader F, Hussein A, Danook S, Mohamad B, Khaleel O. Enhancement of double-pipe heat exchanger effectiveness by using porous media and TiO2 water. CFD Lett 2023;15:31–42. [CrossRef]

[4] Zarda F, Hussein A, Danook S, Mohamad B. Enhancement of thermal efficiency of nanofluid flows in a flat solar collector using CFD. Diagnostyka 2022;23:1–9. [CrossRef]

[5] Hussein A, Najim S, Danook S. Performance improvement of shell and tube heat exchanger by using Fe3O4/water nanofluid. J Therm Eng 2023;9:24–32. [CrossRef]

[6] Ali HHM, Hussein AM, Hussain Allami KM, et al. Evaluation of shell and tube heat exchanger performance by using ZnO/water nanofluids. J Harbin Inst Technol (New Ser) 2023;30:1–11. [CrossRef]

[7] Qader FF, Mohamad B, Hussein AM, Danook SH. Numerical study of heat transfer in circular pipe filled with porous medium. Pollack Period 2023;18:136–141.

[8] Nadi M, Aliehyaei M, Ahmadi A, Turgut OE. Multi-objective particle swarm optimization of the K-type shell and tube heat exchanger (case study). J Therm Eng 2021;7:570–583. [CrossRef]

[9] Peng L, Wang Y. Differential evolution using uniform quasi-opposition for initializing the population. Inf Technol J 2010;9:1629–1634. [CrossRef]

[10] Rahnamayan S, Wang GG, Ventresca M. An intuitive distance-based explanation of opposition-based sampling. Appl Soft Comput 2012;12:2828–2839. [CrossRef]

[11] Rahnamayan S, Tizhoosh HR, Salama MMA. Quasi-oppositional differential evolution. In: Proceedings of IEEE Congress on Evolutionary Computation; 2007. p. 2229–2236. [CrossRef]

[12] Zhang C, Ni ZW, Wu ZJ, Gu LC. A novel swarm model with quasi-oppositional particle. In: Proceedings of International Forum on Information Technology and Applications; 2009. p. 325–330. [CrossRef]

[13] Xu Q, Wang L, He B, Wang N. Modified opposition-based differential evolution for function optimization. J Comput Inf Syst 2011;7:1582–1591.

[14] Sinnott RK. Chemical engineering design: heat transfer equipment. Oxford: Butterworth-Heinemann; 2005.

[15] Aspen Technology. AspenTech. Available at: https://www.aspentech.com. Accessed on December 26, 2025.

[16] Sai JP, Rao BN. Non-dominated sorting genetic algorithm II and particle swarm optimization for design optimization of shell and tube heat exchangers. Int Commun Heat Mass Transf 2022;132:105896. [CrossRef]
[17] Lara-Montaño OD, Gómez-Castro FI, Gutiérrez-Antonio C. Comparison of the performance of different metaheuristic methods for the optimization of shell-and-tube heat exchangers. Comput Chem Eng 2021;144:107076. [CrossRef]
[18] Bell KJ. Final report of the cooperative research program on shell and tube heat exchangers. Newark (DE): University of Delaware, Engineering Experimental Station; 1963.
[19] Seif Z, Ahmadi MB. An opposition-based algorithm for function optimization. Eng Appl Artif Intell 2015;37:293–306. [CrossRef]
[20] Rahnamayan S, Tizhoosh HR, Salama MMA. Opposition-based differential evolution. In: Chakraborty U, editor. Advances in differential evolution. Berlin: Springer; 2008. p. 155–171. [CrossRef]
[21] Caputo AC, Pelagagge PM, Salini P. Heat exchanger design based on economic optimization. Appl Therm Eng 2008;28:1151–1159. [CrossRef]